

Evidence for acceleration of ions to ~ 1 MeV by adiabatic-like reflection at the quasi-perpendicular Earth's bow shock

K. Meziane¹, R. P. Lin¹, G. K. Parks², D. E. Larson¹, S. D. Bale¹, G. M. Mason³, J. R. Dwyer³, and R. P. Lepping⁴

Abstract. On December 6, 1994, during a CIR (Corotating Interaction Region) event, the WIND 3D-Plasma and energetic particle experiment observed a burst (≤ 24 s) of 238-676 keV protons close to the electron foreshock boundary, followed by a 156-236 keV, 101-156 keV and 33-101 keV proton bursts about ~40 s, 65 s and 85 s later, respectively. Similar dispersed bursts of helium with energies between ~50 keV and ~1 MeV followed the proton bursts. During this time, the IMF direction varied slowly with an almost monotonic decrease in θ_{Bn} . The proton energy spectrum is initially peaked at ~350 keV, and progresses to lower energies with time. The proton 3D angular distributions are peaked at ~30° pitch-angle, propagating away from the shock, but they are non-gyrotropic. Finally, we show that the proton energy-spectra as well as the pitch angle distribution agree quantitatively with a model of a single adiabatic reflection of the incident energetic interplanetary ions by the quasi-perpendicular shock.

Introduction

Observations of energetic electron bursts at the Earth's bow shock [Fan *et al.*, 1964] provided the first direct evidence for particle acceleration by a collisionless shock. Velocity-dispersed sheets of electrons from ~ 1 keV to ~ 40 keV have been observed [Anderson *et al.*, 1979] with the more energetic electrons detected closer to the foreshock boundary. Wu [1984] proposed that these energetic electrons are accelerated by a single adiabatic reflection off the strong magnetic field of a nearly perpendicular shock, e.g., the fast-Fermi mechanism. These fast electrons excite Langmuir waves [Filbert and Kellogg, 1979] which provide a tracer of the foreshock boundary.

Field-aligned beams of few keV ions were found traveling upstream from the Earth's bow shock [Asbridge *et al.*, 1968]. These appear to result from the reflection at the shock of a portion of the solar wind ion population [Paschmann *et al.*, 1980]. Later, more energetic 30-100 keV ions were observed upstream of the shock, mostly in the quasi-parallel foreshock region [Lin *et al.*, 1974]. The acceleration of these ions has been attributed to a stochastic Fermi process involving MHD turbulence upstream of the quasi-parallel shock [Lee, 1982; Scholer *et al.*, 1980]. Scholer and Ipavich [1983] and Anagnostopoulos *et al.* [1988] reported bursts

of higher energy, ~150 keV and ~2 MeV ions, respectively, upstream of a quasi-perpendicular shock. Ions up to ~2 MeV energy appear to leak into the upstream medium from the magnetosphere [Sarris *et al.*, 1987; Skoug *et al.*, 1996; Winglee *et al.*, 1996]. Also, incoming ions with velocity smaller than the shock speed can be energized by the so called "shock surfing" mechanism [Lee *et al.*, 1996 and references therein]. Mason *et al.* [1996] recently suggested, from analysis of WIND ion composition measurements, that 30-150 keV/nucleon heavy ions are accelerated by the bow shock during CIR events. Also, Dwyer *et al.* [1997] reported that solar energetic ³He ions are accelerated at the Earth's bow shock.

In this paper, we report the observation of velocity-dispersed bursts of ions up to ~1.4 MeV energy close to the foreshock boundary, occurring during a CIR energetic particle event. The characteristics of these ion bursts are consistent with fast-Fermi acceleration by an adiabatic-like reflection at the near perpendicular shock.

Observations

The observations are from the WIND-3D Plasma and Energetic Particles experiment [Lin *et al.*, 1995]. Three pairs of double-ended telescopes (Solid State Telescopes or SSTs), each with either a pair or triplet of closely stacked silicon semiconductor detectors, provide full 3D coverage with 36°x22.5° angular resolution for electrons above ~20 keV and ions above ~30 keV. One end of each double-ended SST is covered with a Lexan foil whose thickness is chosen to stop protons up to ~ 400 keV in the front 300 micron thick detector; the electrons are essentially unaffected. Electrons above ~ 400 keV will penetrate the front detector and be anti-coincident by the rear detector. The opposite end is open but has a magnet which sweeps away electrons below ~ 400 keV while leaving the ions unaffected. Thus, in the absence of higher energy particles electrons and ions are cleanly separated. When higher energy protons are present (up to 6 MeV stop in the detector), their spectrum is measured by the Open SST and their contribution to the Foil SST can be computed. Heavier ions such as He or CNO require higher energies to penetrate the foil. By comparing the response of the Open and Foil SSTs, some information on the ion species may be obtained.

Solar wind and suprathermal ions up to 30 keV are detected by the ion electrostatic analysers with low (PESA-L) and high (PESA-H) geometrical factor in the 3D Plasma experiment. Suprathermal helium data are provided by the WIND-EPACT experiment [von Rosenvinge *et al.*, 1995]. The electrostatic wave data are provided by the WIND WAVES experiment's thermal noise receiver (TNR) [Bougeret *et al.*, 1995], and the magnetic field data by the WIND MFI experiment [Lepping *et al.*, 1995].

On Dec 6, 1994, WIND was located ~65 R_E upstream of the Earth's bow shock (X_{GSE}=52 R_E, Y_{GSE}=-40 R_E). The IMF magnitude was ~ 15 nT; the IMF direction made an angle of ~ 42° with

¹Space Sciences Laboratory, University of California, Berkeley, CA

²Geophysics Program, University of Washington, Box 351650, Seattle, WA

³Department of Physics, University of Maryland, College Park, MD

⁴Laboratory for Extraterrestrial Physics, NASA/Goddard Space Flight Center, Greenbelt, MD

the solar wind direction. The solar wind velocity was ~ 620 km/s. A CIR event which began at 06:35 UT [Mason *et al.*, 1997], had filled the interplanetary medium at ~1 AU with enhanced fluxes of energetic ions from ~30 keV to >6 MeV/nucleon.

Figure 1 shows observations for the period 08:45-08:54 UT. The SST-Open (panel b) observes a burst of 429-676 keV ions at

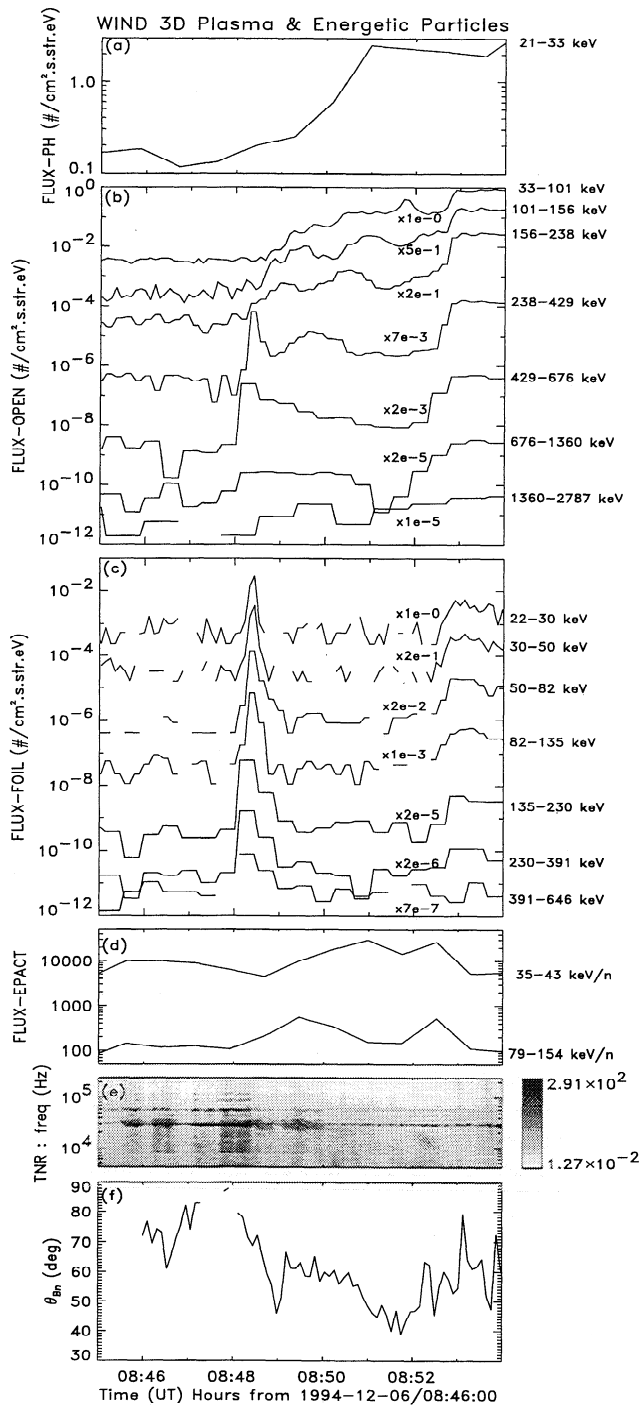


Figure 1. The three top panels display the particle fluxes detected by the PESA-H analyzer (a), and the Open and Foil SSTs (b and c). For clarity the flux in each energy channel has been multiplied by the scaling factors adjacent to each trace. The observed helium flux from the EPACT instrument is shown in panel (d), the electrostatic wave measurements from the WAVE experiment are given in panel (e) and finally the angle θ_{Bn} is shown in panel (f).

08:48:17(± 12 s)UT. In the 238-429 keV channel, a burst of <12s duration occurs in the latter half of that interval and thus could be simultaneous with the 429-676 keV burst. This is followed by bursts in the 156-238 keV, 101-156 keV, and 33-101 keV channels, which occur systematically later at lower energies although there are significant fluctuations, followed by an increase in the 27 keV PESA-H channel (panel a) at 08:51 UT. In the Foil SST (panel c) a burst is detected in all energy channels up to ~500 keV, simultaneous with the Open SST 238-676 keV burst. If the Open SST 238-676 keV burst is due to protons, but not heavier ions, then these fluxes of protons penetrating the foil would be generally consistent with the observed Foil burst count rates, although a small flux of tens of keV electrons cannot be ruled out.

A second set of dispersed bursts starts with a broad peak at 238-429 keV centered at 08:49:40 UT (with possible earlier increases in the 429-676 keV and perhaps 676-1360 keV channels that are merged into the first burst) and peaking at later times at lower energies, up to 08:52 UT for the 33-101 keV channel, with perhaps a related increase at 21-33 keV at 08:52:45 UT. Although this burst extends above ~400 keV, it is not accompanied by a response in the Foil SST, implying that it is not due to protons. The EPACT observations (panel d) show that this burst consists of 79-154 keV/n and 35-43 keV/n He, with the higher energy coming first.

The electrostatic wave measurements (panel e) show an intense burst at the plasma frequency, f_p , at ~08:47:50 UT, indicating that the spacecraft had crossed the electron foreshock boundary just before the 429-676 keV proton spike. Assuming straight line extrapolation of the IMF direction measured on WIND, panel f shows the angle θ_{Bn} computed for a model paraboloid-shaped bow shock: $x = a - (y^2 + z^2)/b$, where $a=15 R_E$, $b=86 R_E$, chosen so θ_{Bn} is ~88° at the time of the electrostatic wave burst. θ_{Bn} decreases more or less monotonically to ~60° by 08:50:50 UT, with the exception of the sharp drop centered at ~08:49 UT. The 238-429 keV and 429-676 keV proton bursts occur in a quasi-perpendicular shock geometry, with $\theta_{Bn} \sim 70^\circ$ -75°. The 33-101 keV and 101-156 keV bursts show a dip at the time of the sharp drop in θ_{Bn} .

The 3D angular distributions in the solar wind frame (Figure 2a) for the 238-429 keV and 429-676 keV proton bursts and the 429-676 keV He burst show that these particles are moving away from the shock, peaked not along the IMF but at ~25° angle pitch angle. The FWHM of these ion beams (Fig. 2b) are ~30° for the protons and somewhat broader for the He. The angular distributions are non-gyrotropic and limited to ~180° of gyrophase.

Figure 3 shows the proton energy spectrum (asterisks) in the maximum flux direction at the time of the narrow first burst (08:48:20-48:26 UT). The dashed line is a power-law fit to the pre-burst CIR event energy spectrum (open circles), assuming protons. The burst proton spectrum exhibits a peak around ~350 keV, and there is no significant flux below 198 keV. At later times the peak moves to lower energies.

Discussion

To understand the observed energy dispersion of the protons and helium we first trace the particle trajectories from the WIND spacecraft back to the bow shock. We assume straight IMF lines and a stationary parabolic bow shock with the same model parameters used earlier and take into account the convection of the field lines by the solar wind during the time it takes the particles to travel to the spacecraft. Figure 4a shows the inferred source regions for the peaks of the proton and helium bursts at each energy. The IMF direction at the shock is shown. Note that differ-

WIND-3DP SST OPEN 1994 December 06

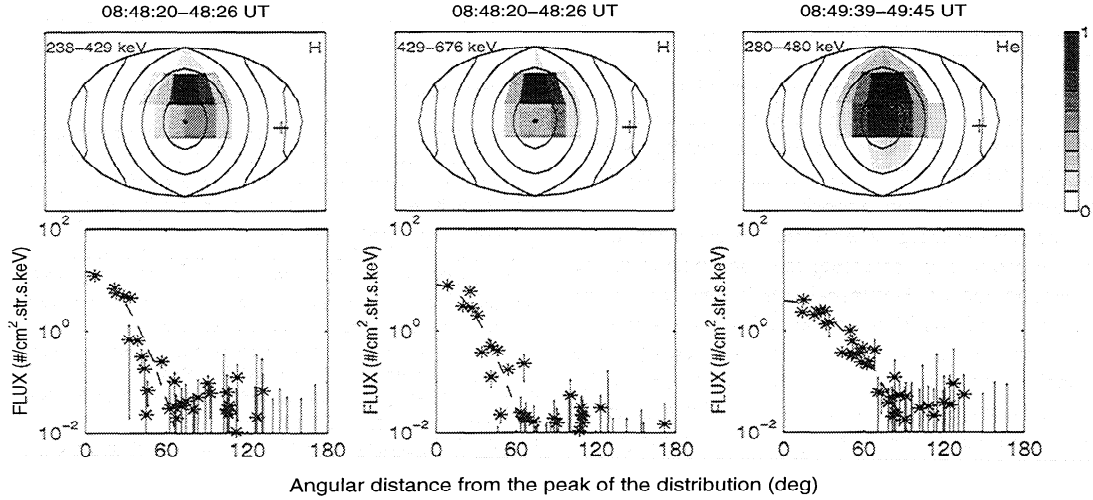


Figure 2. The top panels show 3D proton (a and b) and helium (c) angular distributions sampled in the solar wind frame. The Hammer-Aitoff projection is used to display 4π steradians coverage [Larson et al., 1996]. The **B** vector is located at the center. The solid curves are lines at constant pitch-angle with the interval being 30° . The '+' symbol indicates the solar wind direction. The bottom panels plot flux versus the angle from the peak of the distribution.

ent particle energies and species come from different source regions, indicating that the dispersion is not due to the time of flight from a single source region. The angle θ_{Bn}^* that the magnetic field line makes with the local shock normal at the source region is plotted versus particle velocity in Figure 4b (θ_{Bn}^* differs from θ_{Bn} , which is the angle if the particle velocity is infinite). The angle θ_{Bn}^* ranges between $\sim 60^\circ$ to near 90° . The proton and helium points generally show a systematic decrease with lower velocity, with the exception of the 156-238 keV proton point which occurs during a sudden change of the IMF direction (Fig. 1f).

The dashed line is the shock velocity along the upstream IMF, $V_s = V_{SW} \times (\cos\theta_{Vn}) / (\cos\theta_{Bn}^*)$, where θ_{Vn} is the angle between the solar wind direction and the local shock normal, and V_{SW} is the solar wind velocity. θ_{Vn} is assumed to constant at 42° (it actually varies from $\sim 37^\circ$ to 46°). The velocities of the energetic

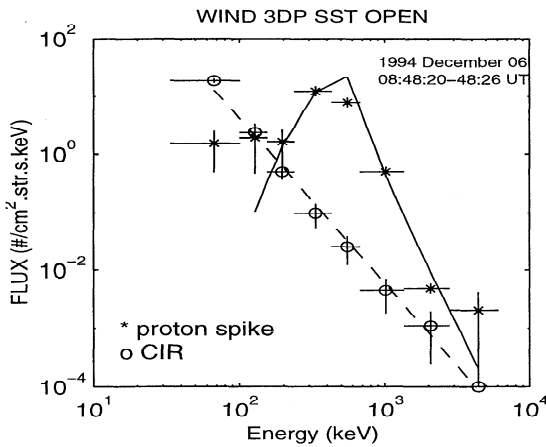
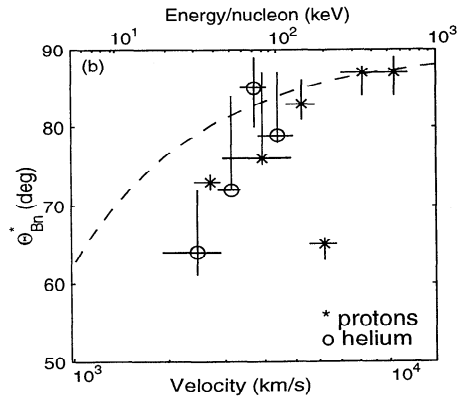
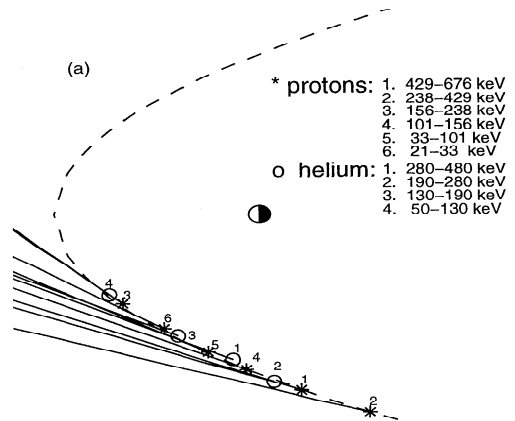


Figure 3. The energy spectrum for the proton burst at 08:48:20-48:26 UT is plotted (asterisks). The dashed line is the best linear fit of the CIR protons measured by the Open SST (circles). The solid curve is the ion spectrum predicted by a single adiabatic reflection of CIR protons for $\theta_{Bn}^* = 84.5^\circ$.

Figure 4. The particle source regions of each burst (Figure 1b) are indicated in the upper panel (a). The lines indicates the IMF directions at the source region (asterisks for protons and circles for He). In (b), the θ_{Bn}^* angle at the source for each burst (assuming a bow shock model, see text) is plotted versus the ion velocity. The dashed curve is the velocity of the shock along the magnetic field.

ions are substantially larger than V_s at the lower energies (Figure 4b). The angular distribution peaks at $\sim 30^\circ$ pitch-angle rather than at 0° , suggesting reflection by the shock. To investigate this further, the jump in field strength across the shock, B_2/B_1 , is needed. This can be estimated using the measured upstream plasma parameters and magnetic field as input to the Rankine-Hugoniot equations together with the shock model. We find that for $\theta_{Bn}^* \sim 75^\circ - 89^\circ$, typical for the 238-676 keV proton bursts, the ratio $B_2/B_1 \approx 3.2 - 3.3$, consistent with a fast mode shock.

The ratio of the particle energy after reflection, E_f , to the initial energy, E_i , can be obtained by assuming the conservation of the magnetic moment in the de Hoffman-Teller frame, where the induced electric field $\mathbf{V} \times \mathbf{B}$ vanishes on both sides of the shock. In the plasma rest frame $E_f/E_i = 1 + 4(\eta^2 - \eta\mu)$ where η is the ratio of the shock velocity V_s to particle velocity V , and μ the cosine of the particle pitch-angle [Decker, 1983]. For a given E_f and pitch-angle μ observed in the burst, E_i can thus be computed. Since the particle space phase density is conserved during the reflection, the flux j_f of the reflected ions is given by: $j_f = (E_f/E_i)j_i$ where j_i is the incident flux. j_i can be obtained for a given E_i from the pre-burst CIR event, whose energy spectrum (assumed protons) is a power law, $j_i = aE_i^{-\gamma}$, with $a=6.3$ and $\gamma=2.84$, and whose pitch-angle distribution (not shown here) appears nearly isotropic with slightly lower flux along the IMF. The resulting energy spectrum, j_f , calculated for $\theta_{Bn}^* \sim 84.5^\circ$ (consistent with the source region) is plotted as the solid curve in Figure 3. The observed burst spectrum matches remarkably well.

The range of pitch-angle distributions for the bursts also agrees with the theoretical prediction for this θ_{Bn}^* and B_2/B_1 . The reflected particles, however, are only observed over $\sim 180^\circ$ of gyrophase angle. When traced back to the shock, the reflected particles' velocities perpendicular to \mathbf{B} generally are directed away from the nose of the shock, as might be expected for the escaping particles' gyromotion to avoid intersecting the shock.

Conclusion

Thin sheets of nearly monoenergetic protons and helium ions are detected streaming away from the quasi-perpendicular region of the Earth's bow shock, systematically dispersed in velocity with the fastest ions found closest to the foreshock boundary. This behavior is very similar to that observed for energetic, few to ~ 100 keV electrons at the foreshock boundary [Anderson et al., 1979], which have been attributed to fast-Fermi acceleration through a single adiabatic reflection by the near perpendicular shock. However, because the ions have gyro-radius much larger than the shock thickness, the adiabaticity is not expected. One possibility is that the Shock Drift Acceleration (SDA) mechanism, where ions drift along the shock and thus gain energy from the $\mathbf{V} \times \mathbf{B}$ convection electric field, could be responsible. Numerical simulations of the SDA process at near perpendicular fast shocks show that it results in a reflected population with the same characteristics as that from a single adiabatic reflection [Decker, 1983]. Our analysis of the observed burst indicates that the ~ 500 keV protons have gained about ~ 400 keV from the acceleration, implying a drift $\sim 10 R_E$ along the shock surface, a distance of order the size of the bow shock itself. The occurrence of such energetic ions accelerated in the quasi-perpendicular Earth's bow shock also depends on the presence of enhanced interplanetary energetic fluxes and high solar wind velocity and strong IMF [Scholer and Ipavich, 1983; Anagnostopoulos et al., 1988]. At quiet times, the interplanetary energetic ion fluxes and the convection electric fields are both much lower, so this type of ion burst will be much less likely to be observed.

Acknowledgments. We are grateful to B. Campbell for his assistance. K. M. thanks Iver Cairns for his valuable comments. Work at UC Berkeley is supported by NASA Grants NAG5-2815 and NAG5-6928.

References

- Anagnostopoulos, G. C., E. T. Sarris, and S. M. Krimigis, Observational test of shock drift and Fermi acceleration on a seed particle population upstream of the earth's bow shock, *J. Geophys. Res.*, **93**, 5541, 1988.
- Anderson, K. A., et al., Thin sheets of energetic electrons upstream from the earth's bow shock, *Geophys. Res. Lett.*, **6**, 401, 1979.
- Asbridge, J. R., S. J. Bame, and I. B. Stong, Outward flow of protons from the earth's bow shock, *J. Geophys. Res.*, **73**, 5777, 1968.
- Bougeret, J. L. et al., WAVES: The radio and plasma wave investigation on the WIND spacecraft, *Space Sci. Reviews*, **71**, 231, 1995.
- Decker, R. B., Formation of shock-spike events at quasi-perpendicular shocks, *J. Geophys. Res.*, **88**, 9959, 1983.
- Dwyer, J. R., et al., Acceleration of solar flare ^3He at the Earth's bow shock, *Geophys. Res. Lett.*, **24**, 61, 1997.
- Fan, C. Y., G. Gloeckler, and J. A. Simpson, Evidence for 20 keV electrons accelerated in the shock transition region beyond the Earth's magnetospheric boundary, *Phys. Rev. Lett.*, **13**, 149, 1964.
- Filbert, P. C., and P. J. Kellogg, Electrostatic noise at the plasma frequency beyond the Earth's bow shock, *J. Geophys. Res.*, **84**, 1369, 1979.
- Larson D. E. et al., Probing the Earth's bow shock with upstream electrons, *Geophys. Res. Lett.*, **23**, 2203, 1996.
- Lee, M. A., Coupled hydromagnetic wave excitation and ion acceleration upstream of the earth's bow shock, *J. Geophys. Res.*, **87**, 5063, 1982.
- Lee, M. A., V. D. Shapiro, and R. Z. Sagdeev, Pickup ion energization by shock surfing, *J. Geophys. Res.*, **101**, 4777, 1996.
- Lepping, R. P. et al., The WIND magnetic field experiment, *Space Sci. Rev.*, **71**, 207, 1995.
- Lin, R. P., C. I. Meng, and K. A. Anderson, 30-to 100 keV protons upstream from the earth's bow shock, *J. Geophys. Res.*, **79**, 489, 1974.
- Lin, R. P. et al., A three-dimensional plasma and energetic particle investigation for the WIND spacecraft, *Space Sci. Rev.*, **71**, 125, 1995.
- Mason, G. M., J. E. Mazur, and T. T. von Roseninge, Energetic heavy ions observed upstream in the Earth's bow shock by STEP/EPACT instrument in WIND, *Geophys. Res. Lett.*, **23**, 1231, 1996.
- Mason, G. M., et al., New spectral and abundance features of interplanetary heavy ions in corotating interaction regions, *Ap. J. Lett.*, **486**, L149, 1997.
- Paschmann, G., et al., Energization of solar wind ions by reflection from the Earth's bow shock, *J. Geophys. Res.*, **85**, 4689, 1980.
- Sarris, E. T., G. C. Anagnostopoulos, and S. M. Krimigis, Simultaneous measurement of energetic ion (≥ 50 keV) and electron (≥ 220 keV) activity upstream of the Earth's bow shock and inside the plasma sheet: Magnetospheric source for the November 3 and December 3, 1977, upstream events, *J. Geophys. Res.*, **92**, 12083, 1987.
- Scholer, M., et al., Conditions for acceleration of energetic ions > 30 keV associated with the earth's bow shock, *J. Geophys. Res.*, **85**, 4602, 1980.
- Scholer, M., and F. M. Ipavich, Energetic ions upstream of the earth's bow shock during an Energetic Storm Particle event, *J. Geophys. Res.*, **88**, 5715, 1983.
- Skoug, R. M. et al., Upstream and magnetosheath energetic ions with energies to ≈ 2 MeV, *Geophys. Res. Lett.*, **23**, 1223, 1996.
- von Roseninge, T. T., et al., The energetic particles: acceleration and transport (EPACT) investigation on the WIND spacecraft, *Space Sci. Rev.*, **71**, 155, 1995.
- Winglee, R. M. et al., Modeling of upstream energetic particle events observed by WIND, *Geophys. Res. Lett.*, **23**, 1227, 1996.
- Wu, C. S., A fast Fermi process: energetic electrons accelerated by a nearly perpendicular bow shock, *J. Geophys. Res.*, **89**, 8857, 1984.

K. Meziane, R. P. Lin, D. E. Larson, and S. D. Bale, Space Sciences Laboratory, University of California, Berkeley, CA 94720.

G. K. Parks, Geophysics Program, University of Washington, Box 351650, Seattle, WA 98195.

G. M. Mason and J. R. Dwyer, Department of Physics, University of Maryland, College Park, MD 20742.

R. P. Lepping, Laboratory for Extraterrestrial Physics, NASA/Goddard Space Flight Center, Greenbelt, MD 20771.

(Received May 24, 1999; revised July 27, 1999; accepted July 30, 1999)